16th World Conference on Earthquake, 16WCEE 2017

Santiago Chile, January 9th to 13th 2017

Paper N° 1057

Registration Code: S-T1461976109

ASSESSING THE SEISMIC HAZARD IN NORTHWESTERN PERU

I. Wong[(1)], S. Pezzopane[(2)], K. Knudsen[(3)], M. Dober[(4)]

[(1)] *Principal Seismologist, URS Corporation (now at Lettis Consultants International), wong@lettisci.com*
[(2)] *Senior Seismic Geologist, URS Corporation (now AECOM), Silvio.Pezzopane@aecom.com*
[(3)] *Senior Seismic Geologist, URS Corporation (now at the U.S. Geological Survey), keithlknudsen@gmail.com*
[(4)] *Project Seismologist, URS Corporation (now AECOM), Mark.Dober@aecom.com*

Abstract

Northwestern Peru is a highly seismically active region situated above the downgoing Nazca plate within the South America subduction zone. Historically, a total of 28 earthquakes of moment magnitude (**M**) 7.0 and greater have occurred in the region, including the 1619 **M** 7.7 to 8 Trujillo earthquake. Several active crustal faults have been identified in the region but likely many more have yet to be discovered.

Probabilistic seismic hazard analysis (PSHA) was performed to assess the hazard in the region as exemplified by the city of Cajamarca. The basic inputs into the PSHA include the seismic source model, ground motion prediction models, and a description of the geologic and geotechnical conditions beneath the site. The seismic source model includes 21 Quaternary-age (active) crustal faults, the South America subduction zone, including both the megathrust and intraslab (Wadati-Benioff) zone, and an areal crustal source zone.

As part of reconnaissance field investigations, several previously recognized crustal faults were characterized as being Quaternary active. The unrecognized La Quinua fault was identified as an active fault capable of generating a maximum earthquake of **M** 6.0 to 6.6. Its slip rate is estimated, however, to be relatively low at less than 0.1 mm/yr. Other local faults characterized include for example, the Carbon, Tapado, Conga, Perol, and Antena faults. A review of the surface-faulting earthquakes in Peru indicates that fault displacements are significantly larger than expected given the mapped fault lengths and empirical relationships. Other significant regional faults include the Chaquilbamba and Bambamarca faults.

The South America subduction zone megathrust is poorly understood in northwestern Peru. Whether it can generate large (**M** > 8.0) megathrust earthquakes is highly uncertain because few large historical earthquakes have been definitely identified as being associated with the megathrust. In this study, we estimate a maximum magnitude for megathrust earthquakes of **M** 8.0 ± 0.5. Its recurrence interval is estimated to be anywhere from 400 to 10,000 years, very uncertain given the lack of data.

State-of-the-art ground motion prediction models were used in the PSHA for the subduction zone and crustal earthquakes. The latter included the recently developed Next Generation of Attenuation (NGA)-West2 models for actively tectonic regions such as Peru. For the subduction zone, we selected three state-of-the-art models. A generic soil Vs30 of 270 m/sec was used in the PSHA.

The hazard in Cajamarca is relatively moderate with PGA values at the building code return periods of 475 and 2475 years of 0.31 and 0.55 g, respectively. The hazard is lower in this part of Peru compared to other regions in the country due to the uncertainty on whether the megathrust to generate very large earthquakes (**M** > 8) because of the flat subduction of the South America plate beneath northwestern Peru.

Keywords: seismic hazards; South American subduction zone; ground motions; Peru

1. Introduction

We have performed a probabilistic seismic hazard analysis (PSHA) of the city of Cajamarca in northwestern Peru. The site region is one of the most seismically active in the world. It is located in the Western Cordillera of the northern Peruvian Andes, approximately 675 km north of Lima, Peru and is also located above the Peruvian portion of the South America subduction zone. The region will be subjected to future strong ground shaking generated by large earthquakes along the subduction zone and numerous other seismic sources.

The primary objective of this study is to estimate the future levels of ground motions in Cajamarca that will be exceeded at a specified probability. Available geologic and seismologic data are used to evaluate and characterize potential seismic sources, the likelihood of earthquakes of various magnitudes occurring on those sources, and the likelihood of the earthquakes producing ground motions over a specified level. It should be noted that there are very significant uncertainties in the characterization of seismic sources and ground motions in Peru due to the limited research in active faulting and strong motion seismology; these uncertainties have been incorporated into the PSHA.

For input into the PSHA, seismic sources need to be defined and ground motion prediction models selected. The seismic sources considered in this analysis include crustal faults, background seismicity, and the South America subduction zone megathrust and Wadati-Benioff (intraslab) zones. For the ground motion prediction models, we used global relationships for all seismic sources.

2. Seismotectonic Setting and Historical Seismicity

Northwestern Peru is located on the westward edge of the South America plate, which overrides the actively subducting Nazca plate (Fig. 1). The South America subduction zone has been the source of some of the largest known earthquakes in the world: the 1868 moment magnitude (**M**) 8.8 Arica, the 1960 **M** 9.5 Southern Chile, 1906 **M** 8.8 Ecuador, and 2010 **M** 8.8 Maule, Chile earthquakes. In addition to these great earthquakes along the interface between the South America and Nazca plates, abundant seismicity occurs in the crust of South America and within the Wadati-Benioff zone of the downgoing Nazca plate (intraslab) (Fig. 1). One of the largest intraslab earthquakes was the devastating 1970 **M** 7.9 earthquake in west-central Peru, which killed 70,000 people and injured 50,000 [1].

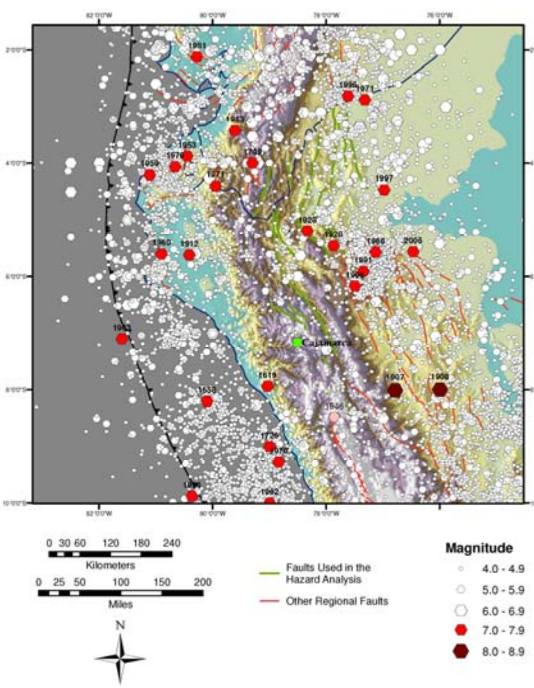

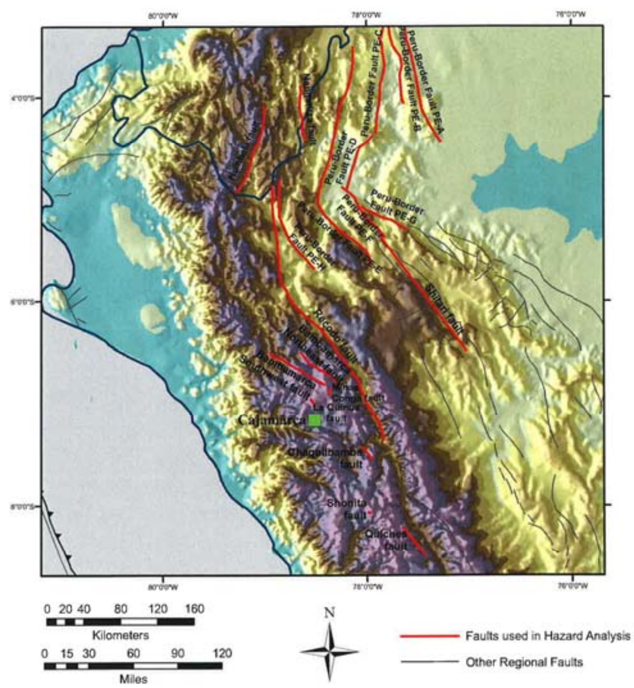

Fig. 1 – Historical seismicity of northern Peru (1541-2010)

Fig. 2 – Crustal faults included in PSHA

The Nazca plate is currently subducting beneath the South America plate at a velocity of about 8 cm/yr [2]. Gutscher *et al.* [2] divide the North Andean portion of the subduction zone beneath the coasts of Colombia, Ecuador, and northern Peru into a number of segments based on subducting slab geometry, seismicity, structure, and volcanism characteristics. At the latitude of Cajamarca, there is relatively flat subduction and no modern arc volcanism. Segments of steep slab subduction and seismicity alternate with aseismic regions and segments of flat subduction [2].

Crustal faults are believed to be abundant in Peru (Fig. 2) given the rapid tectonic deformation within the South America subduction zone as manifested by the high level of seismicity. However, investigations of active faulting have been few in number and limited in scope. A database of known Quaternary faults has been compiled by Macharé *et al.* [3] and updated by Macharé *et al.* [4] (Fig. 2). For many of the faults in the database, very little is known in terms of slip rate, recurrence intervals, and maximum magnitudes due to the lack of geologic and paleoseismic investigations. In addition to shallow crustal faults, both known and unknown, at depths of less than 30 to 40 km the seismic sources in Peru include the South America subduction zone megathrust and the Wadati-Benioff zone (Figs. 1 and 3).

A historical earthquake catalog was compiled for the site region shown on Fig. 1. Primary data sources include catalogs from the U.S. Geological Survey's National Earthquake Information Center (NEIC), Centro Regional de Sismologia para America del Sur (CERESIS), and the Instituto Geofisico del Peru (IGP). The catalog contains more than 9,000 earthquakes spanning the time period from January 1541 to 2010. The catalog can be divided into two time periods: the pre-instrumental period from 1541 to the early 1960s and the instrumental period from then through the present. The instrumental period essentially began with the operation of the Worldwide Standardized Seismographic Network (WWSSN). The first country-wide seismographic coverage came about with the establishment of the Peru National Seismic Network in 1985.

Since 1541, a total of 28 earthquakes of **M** ≥ 7.0 have been recorded and thought to have occurred in the site region (Fig. 1). The largest and most significant in the site region is the 14 February 1619 Trujillo earthquake (Figs. 1 and 3). This earthquake destroyed the city of Trujillo and killed 400 people [5]. The earthquake was felt in Lima and "caused great fear" [5]. No tsunami was reported. Dorbath et al. [5] estimated that the 1619 earthquake was a **M** 7.7 to 8.0 in size and that it is still unknown whether the earthquake was a megathrust or intraslab event but we presume it is not a crustal earthquake.

To evaluate the distribution of earthquakes occurring within the site region, we have examined the historical seismicity to distinguish events occurring within the South American crust and those intraslab events within the subducting Nazca plate (Fig. 1). We have used a focal depth of 30 km to roughly distinguish between the two types of events. Because many of the earthquakes occurred prior to a modern global seismographic network and the National Network, the uncertainties in focal depths are very large. We used the assignment of crustal or intraslab origin in the calculation of earthquake recurrence.

More than 500 earthquakes up to Richter local magnitude (M_L) 4.1 were recorded and located from a 5-year recording of a local seismic network northwest of Cajamarca from 1996 to 2001 [6]. Three groups of earthquakes were observed: (1) shallow earthquakes (< 60 km deep) occurring between the trench and the coastline; (2) shallow events along the trace of the Recodo fault; and (3) intermediate depth events (61 to 350 km deep) distributed throughout the region covered by the temporary network.

An examination of the intraslab seismicity in the site region reveals a pattern of diffuse activity distributed throughout the subducting Nazca plate beneath the site region. Cross-sections of the instrumental seismicity clearly indicate an eastward-dipping seismically active Nazca plate beneath a seismically active South American crust. The plate appears to dip at a shallow angle of about 17° and then steepens at a depth of about 50 km.

3. Active Faults

The extent of active faulting is poorly understood in the Peruvian Andes. According to Costa *et al.* [7], the seismotectonic characteristics of the Central Andes are mainly the consequences of the different subduction geometries along the Nazca plate. Along the Central Andes, particularly north of 33°S, the subducting plate can be grouped into three segments on the basis of the depth and dip of the subducted slab. The site region is above the Peruvian flat-slab segment (latitude 4°S to 14°S) where shallow, moderate magnitude, normal and reverse faulting events are common in the overlying crust, some with associated historical ruptures, for example, along the Chaquilbamba and Quiches faults [3, 8].

A search for late Quaternary faults in the site region was performed using combinations of mainly five data sets: 1) shallow (<10 km in depth) historical crustal seismicity: 2) the Neotectonic Map of Peru [3]; 3)

1:10,000 (local) and 1:100,000, (regional) geological maps; 4) shaded-relief digital elevation models (DEMs) of local and regional topographic data from 1:10,000 orthophoto analysis and Shuttle Radar Mapping (SRTM); and 5) stereographic aerial photography ~1:20,000-scale paper and digital satellite imagery (e.g., mainly LANDSAT, GeoEye, and Quickbird). The search revealed two previously unidentified local faults, the La Quinua fault zone and the Conga fault zone, that show geomorphic evidence for fault scarps in suspected late Quaternary glacial outwash and younger slope deposits.

Fig. 4 shows the geology around the La Quinua fault zone. Fig. 4C is a simplified geologic map from Mallet [9] that shows the La Quinua fault zone and the structural basins west of Yanacocha Cerro. The map shows the principal faults strike mostly northeast and northwest, and Quaternary gravel deposits are coincident with these faults and likely the basin development. Mallet [9] maps the La Quinua fault for ~5 km in length and notes the fault is marked by a scarp 1 to 3 m in height developed in gravel and bedrock. Fig. 4E is an overlay of the map of Mallet [9] onto a satellite image with scarps mapped along the La Quinua fault zone from our field investigations. On the basis of the descriptions of Mallet [9], we infer the La Quinua fault zone and connected fault splays have been involved in recurrent movements since Tertiary time and in latest Quaternary time.

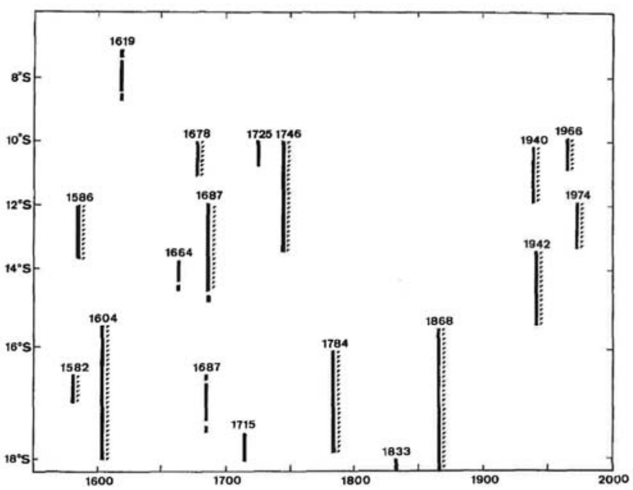

Fig.3

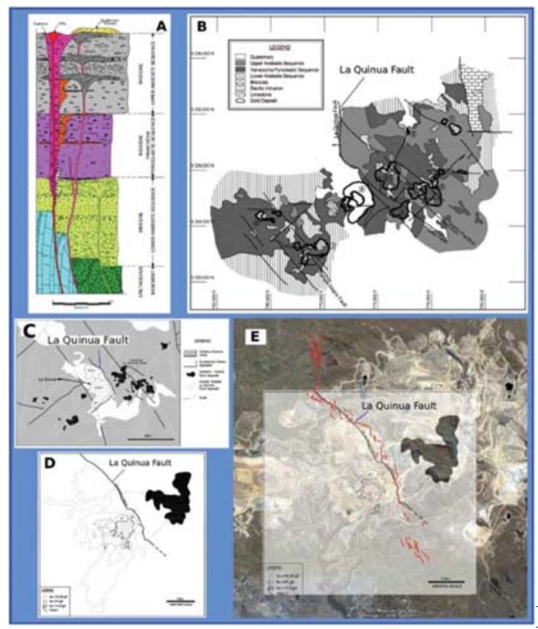

Fig.4

Fig. 3 – Rupture zones of historical earthquakes along South America subduction zone in Peru [9].

Fig. 4 – Stratigraphic column and geologic maps of the La Quina fault and surrounding area: A) generalized stratigraphic column; B) generalized regional geologic map; C) simplified geologic map from Mallet [9]; D) map of La Quinua fault zone; and E) overlay of the map of Mallet [9] onto satellite image

3.1 Field Investigations of the La Quinua Fault

We mapped the La Quinua scarps and other important geologic and geomorphic features. Fig. 5 is an example of the 1996 orthophotography that shows part of the southern end of the La Quinua fault, some of the glacial moraines, and some seeps and springs associated with fault zones. The upper image in Fig. 5A is original; the lower image shows our interpretations of the geomorphic features. In the eastern (right) half of these photos, lateral and recessional moraines and modern stream alluvium and slope colluvium are offset by the La Quinua fault, which strikes north to northwest. The scarp is marked by the dark curving line that cuts across all the topography and landforms, including geologically youthful deposits. The darker streaks on the outwash fan surfaces (center) are young ephemeral stream and slope wash channels, some of which have been entrenched deeply by modern streams that source from artesian springs (Fig. 5). The two sub-parallel, northwest-trending spring alignments (thick red dashed lines) in Fig. 5B are manifestations of the Tapado and Carbon fault zones, which appear to be relatively inactive since glaciation.

The aerial photo and field reconnaissance study revealed that young scarps along the La Quinua fault could be traced confidently on aerial photographs and on the ground (where preserved) a minimum of 6 km. Interpretations of aerial photographs show linear features that we infer are fault traces that continue to the north and south another 1 to 2 km, for a total maximum length of 7.4 km. In places, north of the northern end of the mapped scarp, several geomorphic features such as notched ridges, faceted spurs, artesian spring alignments, and variable stream entrenchment are evidence that the fault zone continues northward some distance beyond what was mapped during our field reconnaissance in this study. No evidence of significant lateral or oblique slip was observed on aerial photography or in the field reconnaissance. The composite scarp geomorphologies indicate at least two paleoearthquakes that we infer occurred probably since the last glacial maximum in late Pleistocene time (~15 to 20 ka).

3.2 Field Investigations in Conga Area

The Conga area are the highlands about 20 km northeast of La Quinua. The limestone mountain belt was intruded and buried by periods of intense volcanism in late Miocene to late Pliocene time (~ 12 to 5 Ma), which filled many of the low-lying eroded areas to create the relatively low-relief topography. Later, the area sustained a long period of erosion from repeated glaciations above ~3,600 m in elevation that resulted in deep incision and karst topography. The history of the glacial stages in this area is poorly known.

QuickBird satellite imagery was digitally draped on the regional topography, and provided slightly better resolution than the conventional aerial photography. Fig. 6A and 6B shows satellite and ground photos of suspected fault features in the Conga area. Fig. 6A is a map view of the three traces along which we found geomorphic evidence of geologically youthful faulting. Fig. 6B is a closer view that shows several north-trending topographic and tonal lineaments that coincide with right-angle bends (offset?) in the course of hillside drainage channels (slope is from left to right). Satellite imagery in Fig. 6A (QuickBird, 2005 Google Earth) show the same oblique west view of a prominent tonal and topographic lineament that notches the hillslope in the central Conga area. Fig. 6E is a photo-mosaic that shows several apparent spring alignments, faceted ridge spurs, bent stream channels, and slope lineaments, all possible evidence of fault scarps.

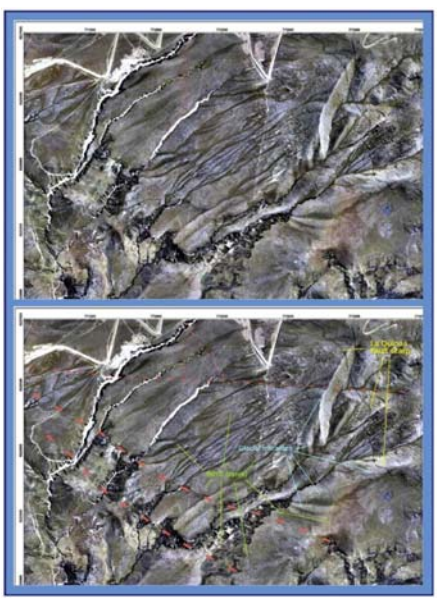
Fig.5

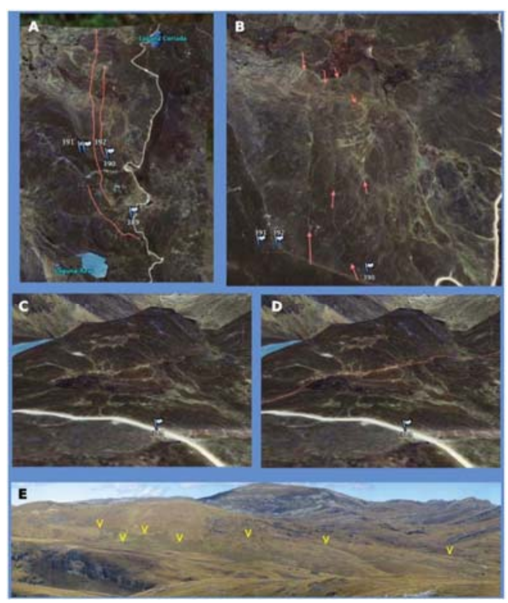
Fig.6

Fig. 5 – 1996 ortho photography and the La Quina fault

Fig. 6 – Vertical and oblique images of suspected fault scarps along Conga fault, from satellite imagery (QuickBird, Google Earth): A) map view of possible fault traces; B) topographic and tonal linears; C) original oblique west view; D) oblique west view with fault interpretations; E) photo-mosaic of spring alignments, faceted ridge spurs, bent stream channels, and linears.

Reconnaissance at several sites in the Conga area confirmed many of the photo interpretations of suspected scarps with evidence such as strong topographic and geomorphic lineaments defined by alignments of numerous side-hill notches, faceted ridge spurs, bent stream channels, and artesian springs. On the basis of available geologic maps, these geomorphic linears are in the vicinity of what is mapped as the Conga fault (unpublished mapping). If one or more of these traces coincides with the Conga fault zone, the fault probably dips to the west with east-side-down displacement. However, the suspected uphill-facing scarps and bent and beheaded stream channels might be more consistent with a component of strike-slip fault motion. Compared to the La Quinua fault scarp geomorphology, the suspected scarps in the Conga fault zone are relatively subdued and more discontinuous. Yet, the aligned geomorphic features in the topography and on hillslope deposits and small slope-wash channels are prominent and continuous, evidence that they are probably no older than the last glacial maximum. For this study, we infer on the basis of available information elsewhere in Peru, that the last glacial maximum in this area is probably no older than Holocene to latest Pleistocene in age (< 20 ky BP). Thus, this study infers that the Conga fault zone is a potential earthquake source on the basis that these geomorphic features represent geologically young fault scarps on hillslope deposits in a high-altitude glaciated region.

Reconnaissance field investigations revealed that the La Quinua fault zone shows abundant evidence of late Pleistocene and Holocene surface displacements in the form of single-event and composite scarps. The Conga fault zone also shows geomorphic evidence for potentially active faulting, although not as clearly expressed as that of the La Quinua fault zone. Results of the fieldwork conclude that the La Quinua fault zone has been active in the late Pleistocene, the Conga fault zone is probably seismogenic, and both fault zones could be sources of moderate-magnitude earthquakes.

4. Seismic Source Characterization

Seismic sources included in the PSHA are crustal faults, the subduction zone megathrust and Wadati-Benioff zone and background crustal seismicity. Potential earthquakes on fault or fold structures that are too small or buried too deep to rupture to the surface are accounted for locally and regionally using a "background" earthquake source zone. Fig. 2 shows the mapped 21 regional crustal faults that we identified as potential seismogenic sources that are included in the PSHA. Not all of these potentially active faults show clear or documented evidence of Quaternary movement, but they are included in the PSHA mostly for completeness and uncertainty evaluations. Two of the more significant of the 21 crustal faults are described below.

4.1 La Quinua Fault

Section 3 describes published information and reconnaissance field mapping that indicates the active La Quinua fault has abundant evidence for composite scarps and recurrent fault slip. The fault is expressed in the young glacial geomorphology of the area and can be mapped for a maximum length of 8 km along a north- to northwest- strike. According to several different empirical relationships between surface rupture length and **M** (e.g., [10]), a rupture length of 8 km is equivalent to Mmax of **M** 6.1 ± 0.3 (Fig. 7A). Magnitude estimates based on empirical relations of **M** and rupture area (from length of 8 km, and downdip rupture widths of 8 km and 16 km) are equivalent to **M** ~5.8 and 6.1, respectively. Given the geomorphic and geologic evidence of repeated offsets, the probability of activity P(a) is assigned 1.0.

In places, the La Quinua fault scarp has a smaller free-face in the middle slope of the scarp face that might represent displacement from the most recent event. This free-face is estimated to range from 0.3 to 0.7 m in height, with a maximum displacement < 1 m. The composite scarps were estimated to range, on average, from 1 to 2 m in height, with a maximum range from 2 to < 3 m for scarps on older deposits. Empirical relationships between average displacement per event and **M** [10] indicate that the average displacements are equivalent to **M** 6.5 and 6.7 (± 0.3), respectively. The range in maximum displacement indicates an **M** 6.5 to 6.7 (± 0.3), same as the average values within uncertainties (measurement and statistical).

A cross-check on the Mmax values is made using the various empirical relationships between potential **M** and estimated source models for La Quinua fault rupture lengths, displacement per events, and rupture areas discussed above. Fig. 7A illustrates the differences using the fault length and displacement for the La Quinua fault and **M** relations. Fig. 7A shows the La Quinua length and displacement data plotted with global empirical relationships between rupture length (bottom axis and solid blue lines), average and maximum displacement per event (top axis, dashed brown lines), and **M** from Wells and Coppersmith [10]. The La Quinua fault length of 8 km corresponds to **M** 6.1 ± 0.3, whereas the displacement data indicate **M** 6.6 ± 0.3.

Fig. 7B shows the length and maximum displacement data for the La Quinua fault zone as well as rupture data from four historical earthquakes in Peru on a plot with the empirical relationships between rupture length (bottom x-axis, solid line), displacement per event (top x-axis, dashed line), and **M** (y-axis) from Wells and Coppersmith [10]. Three events are selected from the database of Wells and Coppersmith [10]. These are the 1946 **M** 7.3 Ancash earthquake; the 1969 **M** 6.1 Pariahuanca event; and the 1986 **M** 5.2 Cuzco earthquake. Also shown are geological and seismological parameters for the Chaquilbamba fault, which may have ruptured in 1937 [3, 11]. In Fig. 7B, the first initial of each event is used with subscript D or L for the rupture displacement or length (e.g., C_D and C_L), respectively, plotted at the relative position on the lines of Wells and Coppersmith [10]. Grey ellipses indicate the La Quinua fault data from Fig. 7A. Points with subscript **M** show the seismological magnitude determined for the event with uncertainty ellipse and a horizontal line that ranges from the L to the D magnitude values. For each event, note the considerable scatter in the three different parameters, which are not completely independent. Ideally they should plot in a horizontal line with the magnitude (intensity) between and connecting the rupture parameters (i.e., 1969 event).

Fig. 7B shows two noteworthy results. First, for all four historical Peruvian earthquakes, and apparently for the La Quinua fault, the maximum rupture displacements are larger than what would be predicted from the rupture lengths (e.g., **M** derived from C_D is greater than **M** from C_L). The differences correspond to as much as 0.5 **M** unit. Fig. 7B shows that compared to the historical data, the “Peruvian” fault ruptures have to double or triple in length in order to match their relatively large surface displacements. Second, Fig. 7B shows that the La Quinua fault length and maximum displacement data have similar scatter as other Peruvian historical earthquakes. Note that the **M** 5.2 Cuzco event and the 1937 Chaquilbamba event have small seismological **M** for the rupture parameters. Also for the Pariahuanca and Ancash events, the **M** values calculated from the geological data vary considerably from the seismological **M** values. In both cases, the differences are as much as ± 0.5 **M**. These examples demonstrate how considerable uncertainties are inherent in the estimation of **M**max from geological faulting parameters. On the basis of the various data shown in Fig. 7B and the fault length and displacement data, a preferred **M**max for the La Quinua fault zone is **M** 6.3 ± 0.3, instead of **M** 6.1 ± 0.3 derived solely from fault length (8 km) or **M** 6.6 ± 0.3 from only the scarp displacement data.

For seismic hazard input, preferably the late Quaternary to Holocene record of displacement is used to derive the fault slip rate, which is the cumulative fault offset divided by the age of the offset units. If the total 200 m of stratigraphic separation in the glacial gravel sequence is considered to be “seismogenic” fault slip that occurred in a time period of 50 ka to say, 200 ka, then the maximum slip rate is ~ 1 to 4 mm/yr. This rate is extraordinarily high for a small, isolated fault like the La Quinua fault, compared to almost any other analogous normal fault in the world, and we suspect the maximum long-term (Tertiary to late Quaternary) slip rate is much less than 1 mm/yr. The single event and composite scarps along the fault confidently represent at least one paleoearthquake, and possibly two events in deposits that are as young as Holocene and probably not older than latest Pleistocene in age. The glacial history and stratigraphy in this area have not been studied, and, to our knowledge, little work has been done beyond that of Mallet [9]. Our preferred model for the La Quinua fault uses **M** 6.3 ± 0.3 earthquakes that produce average displacements per event that range from 0.3 to 0.6 m and have average recurrence intervals that range from 10 to 20 ka, consistent with an average slip rate of ~0.035 ± 0.025 mm/yr. This model is consistent with the surface expression of what we interpret to be average single-event scarps observed in the field reconnaissance and with our preferred age ranges for the offset glacial deposits (Section 3).

4.2 Chaquilbamba Fault

The Chaquilbamba fault is recognized on the Neotectonic Map of Peru [3] and in regional compilations of active faults in South America [8]. The Chaquilbamba fault according to Macharé *et al.* [3], strikes N40°W and has a mapped length of 16 km with scarps as much as 6 to 10 m in height having a fresh free face ~ 1 m in height [11].

Two earthquakes in 1937 were located in the vicinity of the Chaquilbamba fault on the basis of written accounts and intensity information. Bellier *et al*. [11] associated the 1937 events with possible surface rupture along the Chaquilbamba fault, given the fresh-looking free face ~1 m in height. Bellier *et al*. [11] mapped and trenched the Chaquilbamba fault about 13 km south-southeast of Cajabama along the western edge of a prominent range of folded marine sediments. Bellier *et al*. [11] map scarps on the side-slopes and crests of the lateral moraines that average 6 to 8 m in height, with the tallest as much as 10 m. They speculate the scarps are related to two paleoearthquakes that are ~12,000 yr BP and older than 12,000 yr BP in age, respectively.

According to the Peru fault database, the slip rate is "unknown, probably < 1 mm/yr," and recurrence intervals are "unknown" [3]. A slip rate of 0.3 to 0.8 mm/yr is calculated given 6 to 10 m of slip since ~12 to 18 ka. These rates are an overestimate if the displacements from the 1937 earthquakes are included because we do not know when the seismic cycle began. We prefer a model that assumes displacements per event of 0.5 to 1.0 m (consistent with displacement per event calculated from a rupture length of 16 km) that have recurrence intervals of ~ 2 to 5 ka, consistent with slip rates of ~ 0.1 to 0.5 mm/yr. Our preferred slip rate is 0.1 ± 0.2 mm/yr, which assumes that some portion of the scarp is associated with the 1937 earthquake and that perhaps some portion of the scarp may be preserved from the early stages or before the last glacial maximum, the age of which is poorly known. We infer a maximum rupture length of 16 km and no segmentation, which corresponds to **M** 6.5 ± 0.3, in line with **M** derived from a maximum displacement of ~1 m, like the free face.

4.3 Crustal Background Seismicity

Background or random earthquakes are those events that occur on buried or hidden faults without an apparent association with a known or identified tectonic feature. Within the crust of the site region, seismicity is distributed diffusely with no clear relationships with any geologic structures with the exception of the Recodo fault. In northwestern Peru, there are undoubtedly undiscovered faults that are not buried but have geomorphic expression and are capable of producing surface-faulting earthquakes. The hazard from such sources is incorporated into the PSHA through inclusion of an areal source zone and Gaussian smoothing, weighted equally. The latter was done with a spatial window of 15 km to incorporate a degree of stationarity. The cell size used to calculate the hazard was 0.2 degrees. Minimum magnitude was **M** 3.0.

We estimate the Mmax for the background earthquake to be **M** 6.8 ± 0.3. It is likely that earthquakes larger that this value will be accompanied by surface rupture and thus repeated events of this size will produce recognizable fault-related geomorphic features at the earth's surface. This Mmax is larger than the typical values of **M** 6.5 to 6.7 but the crust is above average in thickness in northwestern Peru (> 20 km) in which larger earthquakes could occur without surface faulting.

In order to estimate probabilistic ground motions for the site, recurrence parameters are required for the background seismicity occurring within the Andean zone of the South American crust as well as for the intraslab earthquakes within the subducting Nazca plate. Earthquakes in the historical catalog dating back to 1541 were used in the recurrence estimates. Earthquakes shallower than 30 km were considered to be crustal events. Deeper events were generally considered to be intraslab in origin. It is difficult to distinguish earthquakes occurring on the megathrust because of the uncertainties in the hypocentral depths and the megathrust geometry. Also, even with accurate locations and a well-resolved megathrust, focal mechanism data would still be needed to differentiate between megathrust and intraslab earthquakes.

The recurrence relationships were estimated following the maximum likelihood procedure developed by Weichert [12] and estimated completeness intervals for the region. The relationships are in the form of the truncated exponential distribution for the occurrence of independent earthquakes. Dependent events, foreshocks, aftershocks, or smaller events within an earthquake swarm, were identified using the procedure adopted from Youngs *et al.* [13]. The resulting catalog for 133 independent crustal events was then used to develop the recurrence relationships.

The number of earthquakes was normalized on an annual basis and per unit area (km^2). The resulting recurrence relationship for crustal earthquakes, assuming the usual form of the Gutenberg-Richter relationship of log N = a – *b*M is fairly well constrained except at larger magnitudes. Hence we evaluated the goodness-of-fit with the number of **M** ≥ 7.0 crustal events and adopted two models for the recurrence. They predict weighted recurrence intervals for **M** 6.0 and greater and **M** 7.0 and greater earthquakes of about 20 and 300 years, respectively, for the Andean crustal seismic zone.

4.4 Megathrust

We have modeled both the megathrust and Wadati-Benioff intraslab zones in the PSHA using the geometry shown in Tavera *et al.* [6]. As described earlier, the largest earthquake to possibly rupture the plate boundary of the South America subduction zone beneath the site region was the 1619 Trujillo earthquake (**M** 7.7 to 8) (Fig. 1). The observation that no tsunami was generated raises doubt on whether the event occurred on the megathrust. Two smaller earthquakes in 1960 and 1996 occurred on the megathrust. This portion of the South America subduction zone beneath Peru undergoes flat subduction and its potential for generating great earthquakes (**M** ≥ 8.0) is poorly understood. Nishenko [14] calls this portion of the subduction zone the Chimbote-Guayaquil segment and its ends are defined by the intersection of the Carnegie Ridge and Mendaña fracture zone. Its length is 900 km long. Nishenko [14] characterized this segment as having no historical great earthquakes. Both Pelayo and Wiens [15] and Bourgeois *et al.* [16] concluded that the subduction zone beneath northern Peru is weakly coupled and that convergence is largely aseismic based on examinations of the 1960 and 1996 earthquakes and their tsunamis.

Bourgois *et al.* [17] examined the uplift of marine terraces along the coast of northern Peru between the latitudes of 3.5° and 7.5°S. Their results indicate that the uplift rates in the past 200,000 years range from 10 to 20 mm/yr. Such very high uplift rates would require that the subduction zone megathrust is highly coupled and hence capable of generating great earthquakes [17]. They identify a sequence of 16 “major” earthquakes in the past 20,000 to 23,000 years at Cabo Blanco, which would suggest a recurrence interval of 1,250 to 1,437 years. However, Pedoja *et al.* [18] estimate mean uplift rates of the marine terraces of only 0.12 to 0.27 mm/yr for this same section of the Peruvian Coast. The low rates estimated by Pedoja *et al.* [18] would indicate weak coupling along the megathrust and either long recurrence intervals between great earthquakes or the absence of such events.

Pedoja (University of Caen, written communication, 2011) argues that if the uplift proposed by Bourgois *et al.* [17] is coseismic in nature due to major earthquakes, evidence of such events should be present north and south of the area they investigated but no such sites have been found. Also, the relative coastal stability observed in the second half of the Holocene as evidenced by other geomorphic markers is in contrast to a model that proposes high rates of coastal uplift. Finally, Pedoja argues that because only 5% of coseismic uplift is actually preserved and measurable along the coast in individual uplifts, the 9 m of uplift preserved at Cabo Blanco would actually translate to 180 m of instantaneous coseismic uplift. Such uplift is more than two orders of magnitude higher than what has been observed in Sumatra, the 1960 Chilean coastal area or any other known Holocene earthquake. Such coseismic uplift is clearly not realistic (Pedoja, University of Caen, written communication, 2011). Although there is considerable uncertainty on whether this portion of the Peru subduction zone is capable of generating great earthquakes (**M** ≥ 8.0), smaller megathrust events have been observed. Hence we adopt a P(a) of 1.0.

The areal extent of the potential megathrust rupture plane modeled in the PSHA has been defined by the segment boundaries of Nishenko [19]. It is unlikely that the whole segment could rupture in a single great earthquake. We assign a Mmax distribution of **M** 8.0 ± 0.5. The plate dips at an angle of about 10° ± 5°, which we used to define the approximate eastern boundary of the rupture zone. This portrayal generally agrees with the contemporary seismicity. The maximum depth of the seismogenic megathrust is uncertain. We model the geometry so the maximum depth reaches 20, 30, and 40 km weighted 0.4, 0.4, and 0.2, respectively. The value of 40 km is a typical maximum depth for many subduction zones. Based on the dip and the approximate 40 km depth of the seismogenic portion of the plate interface, the shortest distance between Cajamarca and the potential rupture plane of a megathrust earthquake is about 90 km.

Subduction of the “massive” Carnegie Ridge complex could lead to greater than average recurrence intervals [14]. Based on the observation that no megathrust earthquake of **M** ≥ 8.0 has been observed along Chimbote-Guayaquil segment in nearly 400 years with the possible exception of the 1619 event, we adopt recurrence intervals of 400, 1,350, and 10,000 years roughly weighted 0.2, 0.6, and 0.2, respectively. The best estimate value of 1,350 years is the mean recurrence interval from Bourgois *et al*. [17]. The very long interval of 10,000 years roughly equivalent to the Holocene period is to acknowledge the observation that **M** ≥ 8.0 events are unlikely. We assumed a weight of 1.0 for the maximum magnitude recurrence model assuming that the segment only ruptures in characteristic earthquakes as observed in many subduction zones worldwide. A global average *b*-value of 1.0 ± 0.1 was adopted given the lack of a region-specific value.

4.5 Wadati-Benioff Zone

Based on the 1970 **M** 7.9 event, the intraslab earthquake within the subducting Nazca plate has been assumed to have a Mmax of **M** 7.75 ± 0.25 beneath the site region. If the 1619 earthquake was a slab event, its size is consistent with this range. The plate thickness was assumed to be 45 ± 10 km. The intraslab zones are modeled as a series of 15-km thick staircasing blocks of varying width depending on the along-strike length of the zone, to approximate the 10 degree-dipping Nazca plate.

The recurrence for the Wadati-Benioff zone was calculated in the same manner as the Andean crustal zone. There were 855 independent earthquakes used in the recurrence estimates. There was uncertainty in the number of **M** ≥ 7.0 intraslab events and so the recurrence was calculated assuming 10 and 14 events. The difference in recurrence was insignificant. The recurrence rates predict a **M** ≥ 7.0 earthquake every 25 years in the site region.

5. Ground Motion Prediction Models

In this evaluation, the recently developed PEER NGA-West2 models for the crustal earthquakes in tectonically active regions such as Peru by Abrahamson *et al*. [20], Chiou and Youngs [21], Campbell and Bozorgnia [22], and Boore *et al*. [23] were used in the PSHA. We are unaware of any ground motion prediction models for crustal earthquakes that have been developed for Peru. For the megathrust and intraslab earthquakes, we have used the models of Abrahamson *et al*. [24], Zhao *et al.* [25], and Atkinson and Boore [26] based on the criteria of Arango *et al.* [27]. Models were equally weighted in the PSHA for both the megathrust and intraslab. A generic soil Vs30 of 270 m/sec was used in the PSHA.

6. Hazard Results

The results of the PSHA of the Cajamarca site are presented in terms of ground motion as a function of annual exceedance probability. This probability is the reciprocal of the average return period. At two building code return periods of 475 and 2475 years (10% and 2% exceedance in 50 years), the PGA values are 0.31 and 0.55 g., respectively Fig. 8 shows the seismic source contributions to the PGA hazard. The intraslab zone earthquakes control the hazard at the site at return periods greater than a few hundred years. The crustal background seismicity is also a significant contributor. At 1.0 sec SA, both seismic sources contribute almost equally to the hazard at all the sites. The somewhat surprisingly moderate seismic hazard in Cajamarca compared to other regions in Peru is due to the uncertainty in the subduction zone megathrust potential for generating large (**M** > 8) earthquakes resulting from the flat subduction beneath the site region.

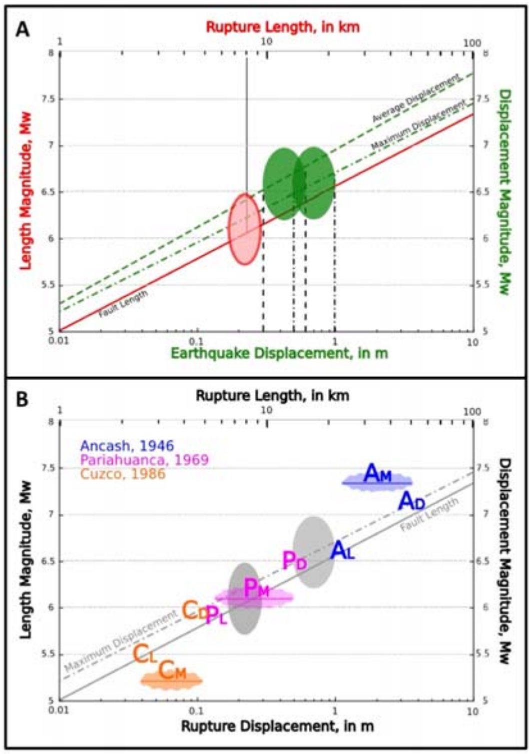

Fig.7

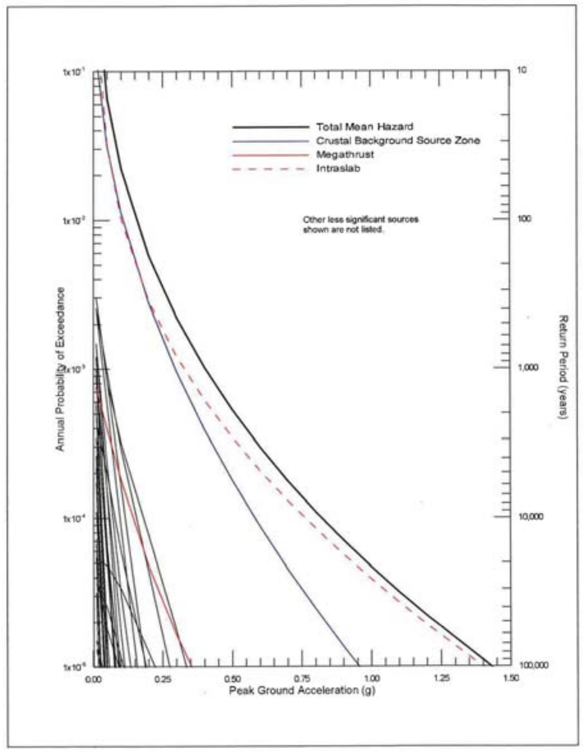

Fig.8

Fig. 7A – Fault length and displacement of La Quina Fault and **M** relations
Fig. 7B – Fault parameters and M relations for selected historical Peruvian earthquakes with La Quina fault

Fig. 8 – Seismic source contributions to PGA hazard in Cajamarca

7. Acknowledgements

Our appreciation to Julia Phillips, Claire Unruh, and Melinda Lee for their assistance in the preparation of this paper. Our study benefited greatly from reviews by Jorge Alva Hurtado, Jose Macharé, and Michael Machette.

8. References

[1] Beck SL and Ruff LJ (1989): Great earthquakes and subduction along the Peru trench. *Physics of the Earth and Planetary Interiors*, **57**(3-4), 199-224.

[2] Gutscher MA, Malavieille J, Lallemand S, and Collot JY (1999): Tectonic segmentation of the North Andean margin: Impact of the Carnegie Ridge collision. *Earth and Planetary Science Letters*, **168**(3-4), 255–270.

[3] Macharé J, Fenton CH, Machette MN, Lavenu A, Costa C, and Dart RL (2003): Database and map of Quaternary faults and folds in Peru and its Offshore Region: U.S., Geological Survey Open-File Report 03-451.

[4] Macharé J, Audin L, Benavente C, Saillard M, Regard V, and Carretier S (2008): Compressive active fault systems along the Central Andean piedmont. *7th International Symposium on Andean Geodynamics (ISAG 2008, Nice),* Extended Abstracts, p. 295-297.

[5] Dorbath L, Cisternas A, and Dorbath C (1990): Assessment of the size of large and great historical earthquakes in Peru. *Bulletin of the Seismological Society of America*, **80**(3), 551-576.

[6] Tavera H, Vilca R, and Marin G (2006): Inferences on the geometry of the Nazca plate in northwestern Peru based on data collected by a local seismograph network. *Earth Science Research Journal*, **10**(1), 15-24.

[7] Costa CH, Audemard M, F.A., Bezerra FHR, Lavenu A, Machette MN, and París G (2006): An overview of the main Quaternary deformation of South America. *Rev. Asoc. Geol. Argent.*, **61**(4), 461-479.

[8] Doser DI (1987): The Ancash Peru earthquake of November 10, 1946-Evidence for low-angle normal faulting in the high Andes of northern Peru. *Geophysical Journal International*, **91**(1), 57-71.

[9] Mallet PM (2002): Geology and mineralization of the La Quinua gold deposit, Yanacocha District, Northern Peru, *in* XI Congreso Peruano de Geologia, Trabajos Cientificos, Sociedad Geologica del Peru, 18 p.

[10] Wells DL and Coppersmith KJ (1994): New empirical relationships among magnitude, rupture length, rupture width, rupture area, and surface displacement. *Bulletin of the Seismological Society of America*, **84**(4), 974-1002.

[11] Bellier O, Sebrier M, Fourtanier E, Gasse F, and Robles I (1989): Late Cenozoic evolution of the E-W striking Cajamarca deflection in the Namora basin (Andes of Northern Peru). *Annales Tectonicae*, **3**, 77-98.

[12] Weichert DH (1980): Estimation of the earthquake recurrence parameters for unequal observation periods for different magnitudes. *Bulletin of the Seismological Society of America*, **70**(4), 1337-1346.

[13] Youngs RR, Swan FH, Power MS, Schwartz DP, and Green RK (2000): Probabilistic analysis of earthquake ground shaking hazard along the Wasatch Front, Utah, *in* P.L. Gori and W.W. Hays (eds.), Assessment of Regional Earthquake Hazards and Risk Along the Wasatch Front, Utah: *U.S. Geological Survey Professional Paper 1500-K-R*, p. M1-M74.

[14] Nishenko SP (1991): Circum-Pacific seismic potential 1989-1999. *Pure and Applied Geophysics*, **135**(2), 169-259.

[15] Pelayo AM and Wiens DA (1990): The November 20, 1960 Peru tsunami earthquake: source mechanism of a slow event. *Geophysical Research Letters*, **17**(6), 661-664.

[16] Bourgeois J, Petroff C, Yeh H, Titov V, Synolakis CE, Benson B, Kuroiwa J, Lander J, and Norabuena E (1999): Geological setting, field survey and modeling of the Chimbote, Northern Peru, tsunami of 21 February 1996. *Pure and Applied Geophysics*, **154**(3-4), 513-540.

[17] Bourgois J, Bigot-Cormier F, Bourles D, Braucher R, Dauteuil O, Witt C, and Michaud F (2007): Tectonic record of strain buildup and abrupt coseismic stress release across the northwestern Peru coastal plain, shelf, and continental slope during the past 200 kyr. *Journal of Geophysical Research*, **112**(B4), B04104.

[18] Pedoja K, Ortlieb L, Dumont JF, Lamothe M, Ghaleb B, Auclair M, and Labrousse B (2006): Quaternary coastal uplift along the Talara Arc (Ecuador, Northern Peru) from new marine terrace data. *Marine Geology*, **228**(1-4), 73-91.

[19] Nishenko SP (1985): Seismic potential for large and great interplate earthquakes along the Chilean and southern Peru margins of South America: A quantitative reappraisal. *Journal of Geophysical Research*, **90**(B5), 3589-3615.

[20] Abrahamson NA, Silva WJ and Kamai R (2014): Summary of the ASK14 ground-motion relation for active crustal regions. *Earthquake Spectra*, **30**(3), 1025-1055.

[21] Chiou BSJ and Youngs RR (2014): Update of the Chiou and Youngs NGA ground motion model for average horizontal component of peak ground motion and response spectra. *Earthquake Spectra*, **30**(1), 1117-1153.

[22] Campbell KW and Bozorgnia Y (2014): NGA-West2 ground motion model for the average horizontal components of PGA, PGV, and 5%-damped linear acceleration response spectra. *Earthquake Spectra*, **30**(3), 1087-1115.

[23] Boore DM, Stewart JP, Seyhan E, and Atkinson GM (2014): NGA-West2 equations for predicting PGA, PGV, and 5% damped PSA for shallow crustal earthquakes. *Earthquake Spectra*, **30**(3), 1057-1085.

[24] Abrahamson NA, Gregor N, and Addo K (2016) BCHydro ground motion prediction equations for subduction earthquakes. *Earthquake Spectra*, **32**(1), 23-44.

[25] Zhao JX, Zhang J, Asano A, Ohno Y, Oouchi T, Takahashi T, Ogawa H, Irikura K, Thio HK, Somerville PG, Fukushima Y, and Fukushima Y (2006): Attenuation relations of strong ground motion in Japan using site classification based on predominant period. *Bulletin of the Seismological Society of America*, **96**(3), 898-913.

[26] Atkinson GM and Boore DM (2003): Empirical ground-motion relations for subduction zone earthquakes and their applications to Cascadia and other regions. *Bulletin of the Seismological Society of America*, **93**(4), 1703-1729.

[27] Arango MC, Strasser FO, Bommer JJ, Cepeda JM, Boroschek R, Hernandez DA, and Tavera H (2012): An evaluation of the applicability of current ground-motion models to the South and Central American subduction zones. *Bulletin of the Seismological Society of America*, **102**(1), 143-168.